Exchange interactions in the perovskites $Ca_{1-x}Sr_xMnO_3$ and $RMnO_3$ (R=La,Pr,Sm)

J.-S. Zhou and J. B. Goodenough
Texas Materials Institute, ETC 9.104, University of Texas at Austin, 1 University Station, C2201, Austin, Texas 78712, USA
(Received 3 March 2003; published 5 August 2003)

Measurement of the variation of the Néel temperature T_N with pressure P and the compressibility κ of the orbitally ordered Mn(III)O_3 array of the $RMnO_3$ family (R=La,Pr,Sm) and of the Mn(IV)O_3 array of the $Ca_{1-x}Sr_xMnO_3$ system have enabled the determination for each of a systematic increase in κ, the magnitude of the Bloch parameter $\alpha_B \equiv d\ln T_N/d\ln V$, and T_N with decreasing bending of the (180°-ϕ) Mn-O-Mn bond angles. The data demonstrate that the anomalously high value of $-\alpha_B=5.5$ reported previously for $LaMnO_3$ is not due to orbital order and its attendant anisotropic magnetic order. A higher $|\alpha_B|$ than 3.3 and an increasing compressibility characterize a system on the approach from the localized-electron side to a first-order transition from localized to itinerant electronic behavior. Moreover, the puzzling empirical relationship $T_N \sim \langle\cos^2\phi\rangle$ for the π-bonding Mn(IV)O_3 array is rationalized by dominance of a semicovalent exchange term over the superexchange term in the perturbation theory for the spin-spin interatomic interactions. The data also provide indirect evidence for a transition from in-phase to out-of-phase stacking along the c axis of the (001)-plane orbital ordering that has been predicted by Mizokawa, Khomskii, and Sawatzky.

DOI: 10.1103/PhysRevB.68.054403 PACS number(s): 75.30.Et, 71.27.+a, 71.28.+d, 71.70.Gm

I. INTRODUCTION

Transition-metal oxides may have d^n manifolds and a Fermi energy located between filled, predominantly O $2p$ bands and empty, primarily cation s, p, and—on rare-earth ions—$5d$ bands. This situation allows study of the interatomic d-d interactions without interference from electrons in overlapping, partially filled broad bands.

In the pseudocubic AMO_3 perovskites, a geometric tolerance factor $t \equiv (A\text{-O})/\sqrt{2}\,(M\text{-O})$ provides a measure of the mismatch of the equilibrium (A-O) and (M-O) bond lengths. A $t<1$ is accommodated by cooperative rotations of the $MO_{6/2}$ octahedra that bend the M-O-M bond angles from 180°. A key parameter regulating the strength of the interatomic (180°-ϕ) M-O-M interactions is the angle ϕ. This angle can be modified by isovalent chemical substitutions on the A sites of ions of different ionic radius; smaller A-site cations reduce t to give a larger angle ϕ and therefore a smaller interatomic (180°-ϕ) M-O-M d-d interaction, and the M-O-M interactions are the dominant d-d interactions within the MO_3 array for $3d$-block transition-metal atoms M. In addition, the strength of the (180°-ϕ) M-O-M interactions can also be varied by the application of hydrostatic pressure.

Some single-valent MO_3 arrays retain localized d^n manifolds in which the spin-spin interactions can be described by perturbation theory, whereas other MO_3 arrays have itinerant $3d$ electrons. Moreover, some MO_3 arrays have both localized and itinerant d electrons. For instance, the Fe(IV)O_3 arrays have localized π-bonding t^3 configurations with spin $S=3/2$ coexisting with a single itinerant electron per Fe atom occupying a partially filled σ^* band of e-orbital parentage. In contrast, the Mn(III)O_3 arrays have localized t^3 configurations and a single localized electron per Mn atom of e-orbital parentage occupying a locally distorted octahedral site in which the distortions lift the e-orbital degeneracy (Jahn-Teller distortions).

We report pressure experiments on $RMnO_3$ (R=rare-earth) and $AMnO_3$ (A=alkaline-earth) perovskites that were designed to explore the evolution of the Néel temperature T_N as the localized to itinerant electronic transition is approached from the localized-electron side. In the $RMnO_3$ family, the t^3 configurations on the Mn(III) ions remain localized, and it is the σ-bonding e electrons that approach the transition to itinerant-electron behavior;[1] in the system $Ca_{1-x}Sr_xMnO_3$, it is the π-bonding t^3 configuration that may become delocalized as a result of screening from their nuclei by back transfer of electrons from the oxygen atoms to the empty e orbitals on their neighboring Mn(IV) ions.

Our strategy is based on the observation that the Néel temperatures of localized-electron perovskite antiferromagnets vary as $T_N \sim \langle\cos^2\phi\rangle$, where the average is taken over the three distinguishable (180°-ϕ) M-O-M bonds in an orthorhombic perovskite, the distortion from cubic symmetry being created by cooperative rotations of the corner-shared $MO_{6/2}$ octahedra about a cubic [110] axis. Explanation of the origin of this empirical relation is deferred to the discussion of the $Ca_{1-x}Sr_xMnO_3$ system. Moreover, the perturbation theory for localized spin-spin interatomic interactions predicts a $dT_N/dP>0$, whereas the theory of band antiferromagnetism predicts a $dT_N/dP<0$ (Ref. 2). The observation that $SrCrO_3$ is a Pauli paramagnetic metal and $CaCrO_3$ is an antiferromagnetic insulator with a $dT_N/dP<0$ was interpreted to signal band antiferromagnetism in $CaCrO_3$ on the approach to the transition from localized to itinerant electronic behavior from the itinerant-electron side.[3] Whether it is possible to find a smooth change from a $dT_N/dP<0$ to a $dT_N/dP>0$ has remained an open question, and the recent argument[4] from the virial theorem that the transition from localized to itinerant electronic behavior should be first order suggests that this quest may prove impossible.

In addition, we have calculated the Bloch parameter α_B

$\equiv d \ln T_N / d \ln V$ from our experimental data. Bloch[5] has examined numerous localized-electron antiferromagnets and found the empirical rule $\alpha_B \approx -3.3$. We find a systematic increase in the magnitude of α_B as the transition from localized to itinerant electronic behavior is approached from the localized-electron side in the single-valent AMO_3 perovskites, and we attribute this behavior to the breakdown of the perturbation description of the spin-spin interactions.

The relation $T_N \sim \langle \cos^2 \phi \rangle$ has been predicted for superexchange interactions between σ-bonding orbitals[6] and observed to hold in the perovskite family $R\mathrm{MnO_3}$ where the rare-earth ion R^{3+} is large enough to stabilize the orthorhombic perovskite structure and in the system $\mathrm{Ca_{1-x}Sr_xMnO_3}$ for $0 \leqslant x \leqslant 0.6$ (Ref. 7). In the $R\mathrm{NiO_3}$ family, the linear relationship between T_N and $\langle \cos^2 \phi \rangle$ is interrupted by an intersection of T_N with an insulator-metal transition temperature T_{IM} in the $\mathrm{Sm_{1-x}Nd_xNiO_3}$ system, and a two-phase regime has been found between $\mathrm{SmNiO_3}$ and metallic $\mathrm{LaNiO_3}$ (Ref. 8). The end members with the highest T_N of each series are promising candidates to demonstrate any transition from localized to band antiferromagnetism. The low-spin Ni(III):t^6e^1 configuration has allowed investigation of the transition among only σ-bonding e electrons in the absence of a localized-electron spin on the π-bonding electrons,[8] whereas the $R\mathrm{MnO_3}$ family contains Mn(III):t^3e^1 configurations in which a localized t^3 π-bonding configuration has a spin $S=3/2$. In $\mathrm{LaMnO_3}$, a partial disproportionation $2\mathrm{Mn(III)} = \mathrm{Mn(II)} + \mathrm{Mn(IV)}$ setting in above $T^* = 600$ K on some of the Mn atoms suggested that, in this compound, the e electrons approach the transition to itinerant behavior.[1] However, orbital ordering introduces an anisotropic type-A magnetic order [ferromagnetic (001) planes coupled antiparallel along the c axis], which raises the concern that the anisotropic magnetic order may be responsible for the large value of α_B that we reported.[9] Therefore, we have chosen to investigate other members of the $R\mathrm{MnO_3}$ family in order to demonstrate a systematic trend in the deviation from the Bloch rule with increasing T_N that shows that the anisotropic magnetic order is not the cause of the deviation from the Bloch rule in $\mathrm{LaMnO_3}$.

II. EXPERIMENT

A. High-pressure equipment

The measurements of ac susceptibility and resistivity under pressure were carried out in a self-clamped Be-Cu cylinder with internal primary and secondary coils and silicon oil as the pressure medium. A 5-kHz ac current in the primary coil generates a magnetic field of about 4 Oe at the sample position. The pressure inside the pressure cell was monitored with a manganin pressure manometer. Depending on the signal quality, the measurements of dc susceptibility or resistivity under pressure have been used to track down the pressure dependence of the Néel temperature. Correlation between the dc magnetization and the ac susceptibility, Fig. 1(a), or $d \ln \rho / d(1/T)$ obtained from the temperature dependence of the resistivity $\rho(T)$, Fig. 1(b), are used, respectively, where

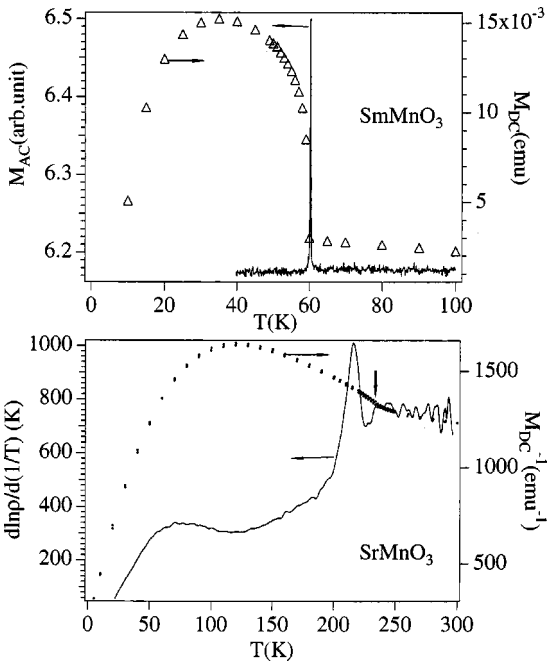

FIG. 1. Temperature dependence of (a) dc magnetization in 5 kOe and ac magnetic susceptibility of $\mathrm{SmMnO_3}$ and (b) dc magnetization in 5 kOe and $d \ln o / d(1/T)$ of resistivity ρ for $\mathrm{SrMnO_3}$.

the sample does or does not exhibit a weak ferromagnetism. The powder diffraction under pressure has been performed in a diamond anvil cell mounted on a four-circle goniometer. The x-ray beam (2.0 kW) is generated from a Mo target in a sealed tube and monochromated by a graphite crystal. Two disks each with a 0.5-mm-diam pin hole are placed at both ends of a collimator (150 mm length) in order to improve parallelism of the beam. NaCl or Au powder mixed with the sample powder and epoxy (no hardener component) is used as the pressure manometer. Powder diffraction peaks show no broadening in pressures up to 5 GPa; they are collected by a Fuji image plate and integrated into a one-dimensional $I \sim 2\theta$ curve with the program FIT2D. The diffraction pattern is analyzed with the program JADE.

B. Material preparation

Single-crystal samples of $R\mathrm{MnO_3}$ (R = La, Pr, Nd, Sm, Eu, Gd, Tb, and Dy) and $\mathrm{CaMnO_3}$ were grown in an infrared-heating image furnace from ceramic bars. A gas flow at 1 atm of argon was used in the crystal growth of $R\mathrm{MnO_3}$ (R = La, Pr, Nd, Sm, and Eu) and air was used for the $R\mathrm{MnO_3}$ (R = Gd and Tb) crystals; 2 atm oxygen pressure was used for growing $\mathrm{CaMnO_3}$. The procedure to synthesize cubic $\mathrm{SrMnO_3}$ has been published previously.[7] All samples are single phase to x-ray powder diffraction. The coefficient dT_N/dP is extremely sensitive to the oxygen stoichiometry in the Mott-Hubbard oxide insulators as has been demonstrated, for example, in $\mathrm{LaTiO_{3\pm\delta}}$ (Ref. 10). Therefore, oxygen stoichiometry has been checked carefully to within 0.1% by measurement of thermoelectric power for $\mathrm{LaMnO_3}$, $\mathrm{PrMnO_3}$, $\mathrm{SmMnO_3}$, and $\mathrm{CaMnO_3}$; it was within 0.3% for $\mathrm{SrMnO_3}$.

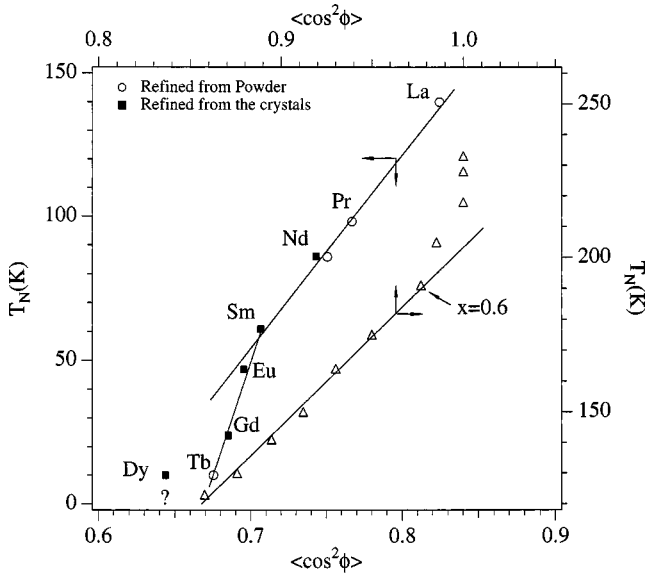

FIG. 2. Néel temperature T_N vs $\langle \cos^2 \phi \rangle$ for the $R\mathrm{MnO_3}$ family (top curve) and the $\mathrm{Ca_{1-x}Sr_xMnO_3}$ system (open triangles) after Ref. 7.

III. RESULTS AND DISCUSSION

A. $R\mathrm{MnO_3}$ perovskites

The anisotropic type-*A* antiferromagnetic order found in $\mathrm{LaMnO_3}$ is a consequence of ordering of the occupied *e* orbital on the Mn(III):t^3e^1 ions[11] below $T_{JT}=750$ K (Ref. 12). The orbital-ordering temperature T_{JT} increases as La is replaced by smaller rare-earth ions.[13] A neutron-diffraction study[14] has revealed a sine-wave magnetic order in $\mathrm{TbMnO_3}$. Although a transition from type-*A* to sine-wave antiferromagnetic order takes place with increasing atomic number of the R^{3+} ion of the $R\mathrm{MnO_3}$ family, refinement of structural data for both single crystals and powders has shown that a $T_N \sim \langle \cos^2 \phi \rangle$ relation holds from $\mathrm{LaMnO_3}$ to $\mathrm{SmMnO_3}$, Fig. 2 (Refs. 15–17), which suggests that a magnetic-ordering transition occurs between $\mathrm{SmMnO_3}$ and $\mathrm{TbMnO_3}$. The La^{3+} ion is the largest R^{3+} ion, and $\mathrm{LaMnO_3}$ has the highest value of T_N in the $R\mathrm{MnO_3}$ family; hydrostatic pressure is required to increase T_N further. We have reported evidence in $\mathrm{LaMnO_3}$ of a disproportionation $2\mathrm{Mn(III)} \rightarrow \mathrm{Mn(II)} + \mathrm{Mn(IV)}$ on some Mn atoms setting in above $T^*=600$ K and increasing discontinuously on heating through T_{JT} (Ref. 1), which we found to be consistent with an unusually high $d \ln T_N/dP = 3.9\times10^{-3}$ $(\mathrm{kbar})^{-1}$ and an $\alpha_B \approx -5.5$ (Ref. 9). In order to test whether this apparent breakdown of the Bloch $\alpha_B \approx -3.3$ rule is due to the anisotropic type-*A* magnetic order, we have investigated the pressure dependence of T_N for isostructural $\mathrm{PrMnO_3}$ and $\mathrm{SmMnO_3}$, which have lower values of T_N.

Figure 3 compares T_N versus *P* for $\mathrm{LaMnO_3}$ and $\mathrm{PrMnO_3}$ over the range $0 < P \leqslant 20$ kbar. Although repeated measurements of $\mathrm{PrMnO_3}$ gave nearly identical curves for T_N versus *P* in the range $0 < P \leqslant 12$ kbar, the second run provided more data points above 12 kbar. In the first run, an average $d \ln T_N/dP = 1.9\times10^{-3}$ $(\mathrm{kbar})^{-1}$ was found within the range $0 < P \leqslant 12$ kbar; an anomalously large value of T_N was found

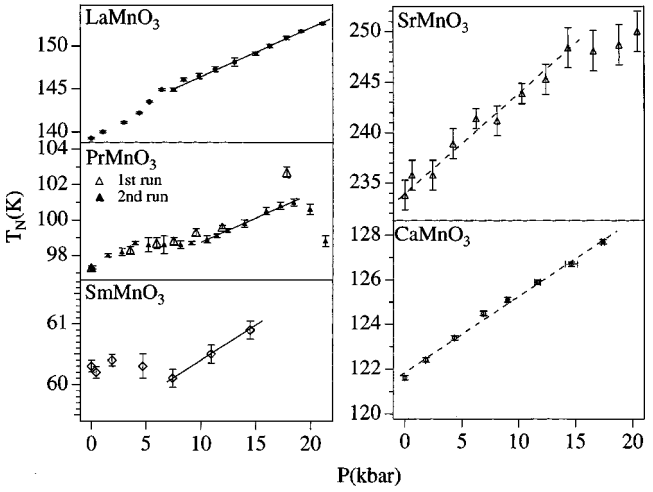

FIG. 3. Néel temperature T_N vs hydrostatic pressure *P* for five manganese-oxide perovskites.

at 17 kbar. The second run gave a $d \ln T_N/dP = 2.6\times10^{-3}$ $(\mathrm{kbar})^{-1}$ in the range $9 < P < 18$ kbar. These values of $d \ln T_N/dP$ are significantly smaller than the $d \ln T_N/dP = 3.9\times10^{-3}$ $(\mathrm{kbar})^{-1}$ of $\mathrm{LaMnO_3}$. More interesting is a change in slope to $dT_N/dP < 0$ above 18 kbar. From these data, it is clear that the effect on T_N of lowering ϕ with hydrostatic pressure is different from that with chemical substitution.

In order to understand the features of the T_N versus *P* curve of $\mathrm{PrMnO_3}$, we measured the structural changes with pressure shown in Fig. 4. The orthorhombic *b* axis in *Pbnm* notation shrinks more dramatically with *P* than either the *a* or *c* axis, which is similar to the lattice-parameter changes of $\mathrm{LaMnO_3}$ under pressure.[18] The factor $s \equiv 2(b-a)/(b+a)$ measures the total structural distortion due to both octahedral-site tilting and the Jahn-Teller-site distortions due to orbital ordering. In $\mathrm{LaMnO_3}$, the site distortions changed little with pressure,[18] so the decrease in the *s* factor from 0.69 to 0.58 under $P=42$ kbar reflects a reduction of the octahedral-site rotations under pressure. Therefore, we assume that changes in the *s* factor in $\mathrm{PrMnO_3}$ under pressure are similarly the result of a reduction of the octahedral-site cooperative rotations under pressure. The *A*-site cations are

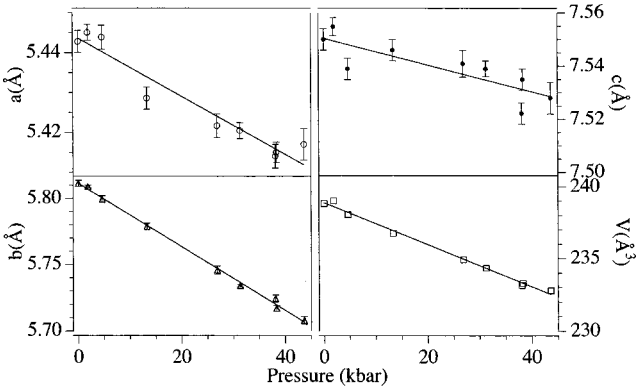

FIG. 4. Pressure dependence of lattice parameters for $\mathrm{PrMnO_3}$. The lines are linear fitting to the data.

displaced from their position in the cubic structure by the cooperative octahedral-site rotations, and a decrease in the *s* factor under pressure reduces the displacement of the Pr^{3+} ions in $PrMnO_3$. Mizokawa *et al.*[19] have calculated that the cooperative orbital ordering responsible for type-*A* antiferromagnetic order may switch from on ''out-of-phase'' arrangement of the (001)-plane orbital ordering in successive (001) planes (*a*-type order) to an ''in-phase'' arrangement (*d*-type order) as the magnitude of the cooperative octahedral-site rotations (their tilting) increases. Although clear experimental evidence to show how the orbitals are ordered in $LaMnO_3$ is not available to us, a significant reduction of the tilting from $PrMnO_3$ to $LaMnO_3$ (Ref. 17) suggests that the *a*-type orbital ordering or a structure having a modulation between the *a* type and *d* type along the *c* axis is stabilized in $LaMnO_3$. An in-phase orbital order in $PrMnO_3$ may change to an out-of-phase orbital order as increasing pressure decreases the octahedral-site tilting. If this phase change occurs and is first order, we should find evidence of a two-phase region in the T_N versus P curve of $PrMnO_3$.

From this perspective, we return to Fig. 3, which shows a plateau in the T_N versus P curve of $PrMnO_3$ in the interval $4<P<11$ kbar, a feature indicative from the Gibbs phase rule of a two-phase region. In support of this inference, the ac susceptibility peak at T_N as in Fig. 2(a) is broadened in this pressure range, which is consistent with the coexistence of two antiferromagnetic phases of slightly different T_N. More compelling is the observation with x-ray diffraction in this pressure range of two phases of close lattice parameters, the volume fraction of the high-pressure phase increasing monotonically with pressure on traversing the pressure range of the plateau in the T_N versus P curve of Fig. 3. Although the resolution of our high-pressure x-ray diffractometer was not sufficient to allow determination of the structural parameters of the two phases, we conclude that the two-phase region probably represents a first-order transition from in-phase to out-of-phase orbital order, each phase giving a type-*A* antiferromagnetic order below a T_N of similar magnitude. As pressure increases the cooperative tilting of the octahedral sites to stabilize the out-of-phase orbital ordering, comparison should be made between the $d\ln T_N/dP$ and the α_B of the high-pressure phase of $PrMnO_3$ in the range $11<P<19$ kbar and of $LaMnO_3$. The pressure dependence of T_N below 7 kbar in $LaMnO_3$ would resemble that of $PrMnO_3$ in a narrow pressure range near 10 kbar. The change to a $dT_N/dP<0$ at $P=19$ kbar in $PrMnO_3$ would appear to signal a transition from localized to itinerant-electron antiferromagnetic order. Although a $dT_N/dP>0$ is found for all pressures in $LaMnO_3$, we note that $PrMnO_3$ has a smaller lattice parameter at ambient pressure and would have a larger overlap integral b_σ than $LaMnO_3$ once the (180°-ϕ) Mn-O-Mn bond angle is straightened by pressure.

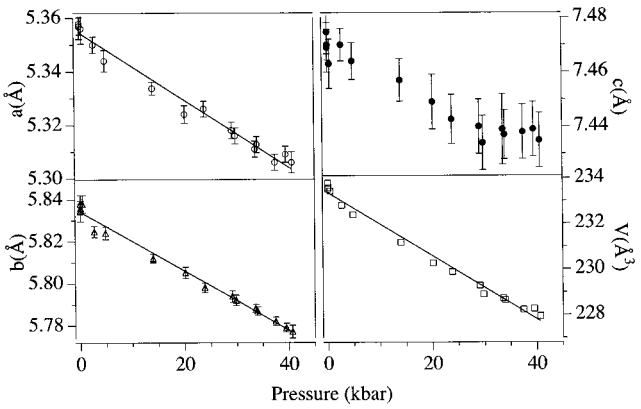

FIG. 5. The same as in Fig. 4 for $SmMnO_3$.

The T_N versus P curve for $SmMnO_3$ in Fig. 3 shows a nearly pressure-independent T_N in the range $0<P<7$ kbar followed by a $d\ln T_N/dP=1.9\times10^{-3}$ $(\text{kbar})^{-1}$. A decrease in the tolerance factor translates to a larger tilting of the $MnO_{6/2}$ octahedra, so any two-phase region associated with a change from in-phase to out-of-phase orbital order should be shifted to higher, not lower, pressures. On the other hand, $SmMnO_3$ appears to be at the threshold of a transition from type-*A* to sine-wave magnetic order as discussed in connection with Fig. 2. Since the phase with sine-wave magnetic order has a slightly larger volume below T_N (Ref. 14), the two-phase region in this case may be associated with a change from sine-wave to type-*A* antiferromagnetic order. Whether the orbital ordering giving type-*A* antiferromagnetic order is in phase or out of phase, the data for $PrMnO_3$ suggest that there is little difference in the values of $d\ln T_N/dP$ for the two types of orbital ordering, so we believe we are justified in comparing the values of $d\ln T_N/dP$ for $LaMnO_3$, $PrMnO_3$, and $SmMnO_3$. From the structural data of Figs. 4 and 5, we obtain the compressibilities and hence the Bloch parameters $|\alpha_B|$ shown in Table I. The α_B for $SmMnO_3$ is comparable to that predicted by Bloch, whereas there is a systematic deviation from the Bloch rule as T_N increases from $SmMnO_3$ to $PrMnO_3$ to $LaMnO_3$. There is no indication that the deviation found is due to the anisotropic magnetic order, and therefore we conclude, as in our earlier paper,[9] that the deviation is due to an approach to the localized to itinerant electronic transition from the localized-electron side in $LaMnO_3$. This conclusion is consistent with the observation of a fluctuating partial disproportionation reaction $2\text{Mn(III)}=\text{Mn(II)}+\text{Mn(IV)}$ above 600 K in $LaMnO_3$.

TABLE I. Parameters measured and coefficient $\alpha=-d\ln T_N/d\ln V$ for the perovskite oxides studied.

	$CaMnO_3$	$SrMnO_3$	$SmMnO_3$	$PrMnO_3$	$LaMnO_3$
$T_N^{-1}dT_N/dP$ $(10^{-3}$ $\text{kbar}^{-1})$	2.79	3.98	1.9	2.9	3.9
$V^{-1}dV/dP$ $(10^{-3}$ $\text{kbar}^{-1})$	0.68	0.71	0.59	0.61	0.71[a]
$\alpha=-d\ln T_N/d\ln V$	4.1	5.6	3.2	4.7	5.5

[a]From Ref. 18.

B. $Ca_{1-x}Sr_xMnO_3$ system

The Mn(IV)O_3 array of the system $Ca_{1-x}Sr_xMnO_3$ contains localized t^3 configurations at the Mn(IV):t^3e^0 ions, and the spin-spin coupling between half-filled orbitals with spin $S=3/2$ is antiferromagnetic to all six near-neighbor Mn(IV) to give type-G antiferromagnetic order. As shown in Fig. 2, a $T_N \sim \langle \cos^2 \phi \rangle$ holds in $Ca_{1-x}Sr_xMnO_3$ for $0 \leqslant x \leqslant 0.6$ where the structure is orthorhombic. The large Sr^{2+} ion increases the tolerance factor, and the cooperative $MnO_{6/2}$ octahedral-site rotations change to give tetragonal symmetry and then cubic symmetry as x increases in the range $0.6 \leqslant x \leqslant 1.0$. The deviation of T_N from a linear dependence on $\langle \cos^2 \phi \rangle$ for $x > 0.6$ is associated with the change from orthorhombic symmetry. Nevertheless, the t^3 configurations remain localized, and the magnitude of $d \ln T_N/dP$ is highest for the compound with the largest T_N in the system, changing from 2.8×10^{-3} $(\text{kbar})^{-1}$ in $CaMnO_3$ to 4.0×10^{-3} $(\text{kbar})^{-1}$ in $SrMnO_3$, Fig. 3. In this system, there is no orbital degeneracy to be removed by a local Jahn-Teller deformation as occurs in the $RMnO_3$ family, and the unusually high $d \ln T_N/dP$ found in the cubic phase of $SrMnO_3$ creates a new puzzle. As can be seen in Fig. 3, a saturation (or plateau) in the T_N versus P curve at $T_N = 250$ K at $P = 15$ kbar appears to signal a phase transition that cannot be related to orbital order and is not expected to reflect a change in the magnetic order unless next-near-neighbor interactions become sufficiently large to induce stabilization of a spiral-spin configuration propagating along a [111] axis.

To begin the discussion, we note that a $T_N \sim \langle \cos^2 \phi \rangle$ for t^3-O-t^3 interactions, as occurs in $Ca_{1-x}Sr_xMnO_3$, does not follow naturally from the Anderson theory of superexchange. In fact, the perturbation theory for interatomic exchange interactions in a single-valent MO_3 array contains two terms: a superexchange term containing the on-site electron-electron Coulomb energy U required to excite an electron from one d^n manifold to another and a semicovalent-exchange term containing the energy Δ to excite an electron from an O $2p$ orbital to the lowest unoccupied d orbital of the d^n manifold. The Néel temperature of an antiferromagnetic is then given by

$$T_N \sim \sum (b^{ca})^4 \Delta^{-2} [U^{-1} + (2\Delta)^{-1}], \quad (1)$$

where b^{ca} is the cation-anion electron-energy transfer integral and the sum Σ is over all virtual charge transfers involved in a pair interaction as well as over all nearest-neighbor interactions. The factor of 2 in the denominator of the semicovalent-exchange term reflects the need to transfer two electrons from the oxygen, one to each neighboring cation, to obtain an interatomic spin-spin interaction between the cations. The semicovalent-exchange mechanism was initially proposed[20] in 1955 and was subsequently given mathematical form by Nesbet.[21,22] After identification of a charge-transfer gap Δ, Geertsman[23] obtained a more explicit formula. Since both terms in Eq. (1) give the same rules for the sign of the exchange interaction,[24] it became customary to apply only the Anderson formulation for a qualitative discussion of the interatomic interactions. However, Sawatzky[25] found it necessary to reintroduce the second term in Eq. (1) to explain the trend of the Néel temperatures in the monoxides. The semicovalent-exchange term was also derived later by Zhang and Rice[26] from a two-band model for La_2CuO_4.

The physics involved in Eq. (1) is quite simple: we illustrate it for the t^3e^0-O-t^3e^0 interactions in a Mn(IV)O_3 array. The Anderson[27] superexchange involves a virtual electron transfer from a half-filled π-bonding t orbital on one atom to a half-filled t orbital on the neighboring Mn(IV) ion. The spin of the transferred electron is conserved, and the Pauli exclusion principle restricts transfer to a state antiparallel to the spin on the acceptor ion. The energies involved in this transfer are b_π^{ca} and U_π. Bending the M-O-M angle has no effect on the overlap integrals involved in one π-bond transfer and a competition between increasing and decreasing overlap of the other π-orbital transfer. The semicovalent transfers involve both the b_π^{ca} and the b_σ^{ca}. The Pauli exclusion principle favors transfer of O $2p_\pi$ electrons antiparallel to the spin on the cations; ferromagnetic intra-atomic exchange favors transfer of O $2p_\sigma$ electrons to the empty e orbitals that are parallel to the Mn(IV)-ion spins. Since the O p_π and O p_σ orbitals are each spin paired, electrons of opposite spin are preferentially transferred to the two neighboring cations overlapping the same O $2p$ orbital. An individual exchange interaction becomes

$$J \sim 4(b_\pi^{ca})^4 \Delta_\pi^{-2} [U_\pi^{-1} + (2\Delta_\pi)^{-1}] + (b_\sigma^{ca})^4 \Delta_{\text{ex}}/\Delta_\sigma^4, \quad (2)$$

where Δ_{ex} is the intraatomic exchange energy. Simple geometric considerations make the σ-bonding overlap integrals $(b_\sigma^{ca})^2/\Delta_\sigma \sim \cos\phi$, so the σ-bond component gives a contribution to T_N that is proportional to $\langle \cos^2 \phi \rangle$. The π-bond component, on the other hand, should have little dependence on ϕ. Therefore, the observation of a $T_N \sim \langle \cos^2 \phi \rangle$ in the system $Ca_{1-x}Sr_xMnO_3$ signals an important semicovalent-exchange component; in fact, a $\Delta \ll U_\pi$ in the $Ca_{1-x}Sr_xMnO_3$ system makes dominant the semicovalent exchange term.

C. Bloch rule

The overlap integral varies with the (M-O) bond length r as r^{-n}, and calculation[28,29] has given $b^{ca} \sim r^{-n}$ with $n = 2.5$–3, which makes $T_N \sim r^{-10} \sim V^{-3.3}$ and the Bloch parameter $\alpha_B \equiv d \ln T_N/d \ln V \approx -3.3$ provided the values of U and Δ do not change with the volume. From the compressibility data measured as in Figs. 4 and 5 and the T_N versus P data of Fig. 3, we obtained the data of Table I. The magnitudes of α_B for $LaMnO_3$ and $SrMnO_3$ are both clearly larger than predicted by the Bloch rule. Moreover, both the compressibility and $-\alpha_B$ are seen to increase systematically with T_N for both the Mn(III)O_3 and Mn(IV)O_3 arrays. This behavior could signal a decrease in Δ_π and/or Δ_σ with increasing pressure with a breakdown of the assumption of a constant U and Δ, which would simply be a breakdown of the mathematical model. On the other hand, it could also signal the influence of a double-well potential for the equilibrium (Mn-O) bond length on the approach to a first-order phase transition. This second option becomes plausible for

$LaMnO_3$ because of the onset of a fluctuating partial disproportionation reaction above $T^* \approx 600$ K. Moreover, the T_N for $SrMnO_3$ saturates above 14 kbar, Fig. 3, which signals the onset of a first-order phase change where there can be no possibility of orbital reordering; the possibility of a first-order change in the O $2p$ admixture in the M-O bonding could, however, enhance next-near-neighbor interactions to induce a change in the antiferromagnetic order. Moreover, the higher compressibility of the $LaMnO_3$ and $SrMnO_3$ crystals is consistent with the approach to the crossover of a double-well potential of the (Mn-O) bond. A similar systematic enhancement of $-\alpha_B$ and compressibility was observed in the $R NiO_3$ family as T_N increases to that of $SmNiO_3$, the compound on the threshold of the transition from localized to itinerant electronic behavior.[8]

In the two-phase region at the crossover from localized to itinerant electronic behavior in the $R NiO_3$ family and in the $La_{1-x}Sr_xMnO_3$ system, the thermal conductivity is strongly suppressed.[8,30] Both the single-valent $R NiO_3$ family and mixed-valent $La_{1-x}Sr_xMnO_3$ system show a complete crossover from localized to itinerant electronic behavior; suppression of the phonon contribution to the thermal conductivity is confined to the crossover region where a dynamic phase segregation is realized by locally cooperative bond-length fluctuations. It is, therefore, significant that the thermal conductivities of $LaMnO_3$ and $SrMnO_3$ are lower than other members of the $R MnO_3$ family or the $Ca_{1-x}Sr_xMnO_3$ system just as was found for $SmNiO_3$, which is known to be at the threshold of the crossover from the localized-electron side.

Finally, a word of caution about extrapolation of these findings to other perovskite systems. For example, the itinerant-electron antiferromagnet $LaTiO_3$ exhibits an unusually high $d \ln T_N/dP = 4.9 \times 10^{-3}$ $(\text{kbar})^{-1}$ (Ref. 10), but T_N decreases as the bending angle ϕ increases until there is a change to ferromagnetic order at $GdTiO_3$ with T_c increasing with ϕ for the heavier rare earths.[31] In this case, competition between antiferromagnetic and ferromagnetic order at the crossover from itinerant-electron antiferromagnetism to ferromagnetic order results from a π^* band that is less than half-filled, and the composition with the highest T_N—viz, $LaTiO_3$—is not at the threshold from localized to itinerant electronic behavior. Broadening of the π^* band of $LaTiO_3$ with pressure lowers the competition from ferromagnetic interactions, thereby raising T_N.

IV. CONCLUSIONS

Investigation of the effect of pressure on the Néel temperature and the compressibility of the orbitally ordered $R MnO_3$ family (R=La,Pr,Sm) and the $Ca_{1-x}Sr_xMnO_3$ system have revealed the following: (1) In the orthorhombic samples, $T_N \sim \langle \cos^2 \phi \rangle$ holds for both the $Mn(III)O_3$ and $Mn(IV)O_3$ arrays; a discontinuous decrease in ϕ on passing from orthorhombic to cubic structure found in $SrMnO_3$ gives rise to a discontinuous increase in T_N. (2) A systematic increase in the magnitude of the Bloch parameter $\alpha_B = d \ln T_N / d \ln V$ with increasing T_N from its normal value $-\alpha_B = 3.3$ to 5.5 and 5.6, respectively, in both the $R MnO_3$ family and $Ca_{1-x}Sr_xMnO_3$ system shows that the anomalously high value of $-\alpha_B$ for $LaMnO_3$ previously reported is not due to the orbital order and the resulting anisotropic magnetic order. (3) Systematic increases in the compressibility and in $|\alpha_B|$ as T_N increases in both the $R MnO_3$ family and the $Ca_{1-x}Sr_xMnO_3$ system are not simply due to a breakdown of the mathematical description of the interatomic interactions; they also reflect the existence of a double-well potential for the equilibrium (Mn-O) bond length on the approach to a first-order crossover from localized to itinerant electronic behavior. (4) Interpretation of the variation of T_N with P is made complex for the $R MnO_3$ family because changes in orbital ordering and in the magnetic order can each give rise to first-order phase changes before any crossover from localized to itinerant electronic behavior occurs. (5) The $T_N \sim \langle \cos^2 \phi \rangle$ dependence found in the orthorhombic structure having $Mn(IV)O_3$ array and the anomalously high $d \ln T_N/dP$ of $SrMnO_3$ both provide fresh evidence for the dominance of the semicovalent-exchange term in perovskites with a charge-transfer gap $\Delta < U_\pi$.

ACKNOWLEDGMENTS

We thank J. Yan for his effort in programming, which made the data transfer in the x-ray diffraction possible, Professor B. Dabrowski for providing the ceramic $SrMnO_3$ sample, and the financial support of the NSF, the TCSUH of Houston, Texas, and the Robert A. Welch Foundation of Houston, Texas.

[1] J.-S. Zhou and J. B. Goodenough, Phys. Rev. B **60**, R15 002 (1999).
[2] J. B. Goodenough, Prog. Solid State Chem. **5**, 145 (1971).
[3] J. B. Goodenough, J. M. Longo, and J. A. Kafalas, Mater. Res. Bull. **3**, 471 (1968).
[4] J. B. Goodenough, Aust. J. Phys. **52**, 155 (1999).
[5] D. Bloch, J. Phys. Chem. Solids **27**, 881 (1966).
[6] C. Boekema, F. Van Der Woude, and G. A. Sawatzky, Int. J. Magn. **3**, 341 (1972).
[7] O. Chmaissem, B. Dabrowski, S. Kolesnik, J. Mais, D. E. Brown, R. Kruk, P. Prior, B. Pyles, and J. D. Jorgensen, Phys. Rev. B **64**, 134412 (2001).
[8] J.-S. Zhou, J. B. Goodenough, and B. Dabrowski, Phys. Rev. B **67**, 020404(R) (2003).
[9] J.-S. Zhou and J. B. Goodenough, Phys. Rev. Lett. **89**, 087201 (2002).
[10] Y. Okada, T. Arima, Y. Tokura, C. Murayama, and N. Mori, Phys. Rev. B **48**, 9677 (1993).
[11] J. B. Goodenough, Phys. Rev. **100**, 564 (1955).
[12] J. Rodriguez-Carvajal, M. Hennion, F. Moussa, A. H. Moudden,

L. Pinsard, and A. Revcolevschi, Phys. Rev. B **57**, R3189 (1998).
[13] J.-S. Zhou and J. B. Goodenough (unpublished).
[14] J. Blasco, C. Ritter, J. García, J. M. de Teresa, J. Pérez-Cacho, and M. R. Ibarra, Phys. Rev. B **62**, 5609 (2000).
[15] T. Mori, K. Aoki, N. Kamegashira, T. Shishido, and T. Fukuda, Mater. Lett. **42**, 387 (2000).
[16] T. Mori, N. Kamagashira, K. Aoki, T. Shishido, and T. Fukuda, Mater. Lett. **54**, 238 (2002).
[17] J. A. Alonso, M. J. Martínez-Lope, M. T. Casais, and M. T. Fernández-Díaz, Inorg. Chem. **39**, 917 (2000).
[18] L. Pinsard-Gaudart, J. Rodríguez-Carvajal, A. Daoud-Aladine, I. Goncharenko, M. Medarde, R. I. Smith, and A. Revcolevschi, Phys. Rev. B **64**, 64426 (2001).
[19] T. Mizokawa, D. I. Khomskii, and G. A. Sawatzky, Phys. Rev. B **60**, 7309 (1999).
[20] J. B. Goodenough and A. L. Loeb, Phys. Rev. **98**, 391 (1955).
[21] R. K. Nesbet, Ann. Phys. (N.Y.) **4**, 87 (1958).
[22] R. K. Nesbet, Phys. Rev. **119**, 658 (1960).
[23] W. Geertsma, Ph.D. thesis, University of Groningen, The Netherlands, 1979.
[24] J. B. Goodenough, *Magnetism and the Chemical Bond* (Interscience-Wiley, New York, 1963).
[25] G. A. Sawatzky, in *Earlier and Recent Aspects of Superconductivity*, edited by J. G. Bednorz and K. A. Muller (Springer-Verlag, Berlin, 1990).
[26] F. C. Zhang and T. M. Rice, Phys. Rev. B **37**, 3759 (1988).
[27] P. W. Anderson, in *Magnetism*, edited by G. J. Rado and H. Suhl (Academic, New York, 1963), Vol. I, Chap. II.
[28] K. N. Shrivastava and V. Jaccarino, Phys. Rev. B **13**, 299 (1976).
[29] D. W. Smith, J. Chem. Phys. **50**, 2784 (1969).
[30] J.-S. Zhou and J. B. Goodenough, Phys. Rev. **64**, 024421 (2001).
[31] Y. Okimoto, T. Katsufui, Y. Okada, T. Arima, and Y. Tokura, Phys. Rev. B **51**, 9581 (1998).